International Journal of Environmental Health Research

ISSN: 0960-3123 (Print) 1369-1619 (Online) Journal homepage: www.tandfonline.com/journals/cije20

Assessing leishmaniasis risk in irrigated lands in Central Tunisia using visible-spectrum remote sensing data

Attila J. Trájer

To cite this article: Attila J. Trájer (02 Mar 2026): Assessing leishmaniasis risk in irrigated lands in Central Tunisia using visible-spectrum remote sensing data, International Journal of Environmental Health Research, DOI: 10.1080/09603123.2026.2639719

To link to this article: https://doi.org/10.1080/09603123.2026.2639719

Published online: 02 Mar 2026.

INTERNATIONAL JOURNAL OF ENVIRONMENTAL HEALTH RESEARCH
https://doi.org/10.1080/09603123.2026.2639719

Taylor & Francis
Taylor & Francis Group

RESEARCH ARTICLE

Assessing leishmaniasis risk in irrigated lands in Central Tunisia using visible-spectrum remote sensing data

Attila J. Trájer

Sustainability Solutions Research Lab, University of Pannonia, Veszprém, Hungary

ABSTRACT

The expansion of irrigation in central Tunisia has reshaped landscapes, creating ecological conditions favourable to *Phlebotomus* sand flies and *Leishmania* transmission, thereby increasing leishmaniasis risk. To assess these dynamics, a geospatial classification and risk-indexing framework was developed that integrates remote sensing, supervised machine learning, and ecological reasoning on vector habitats. The analysis covered three Central Tunisian sites and their narrower environments – Gafsa, Kairouan, and Sidi Bouzid – from 1984 to 2020. Habitat clustering revealed marked spatial and temporal variability in land-cover composition. Low-risk habitats remained dominant, while irrigated high-suitability areas expanded progressively, particularly after the mid-1990s. Semi-natural habitats fluctuated, and very low-risk areas remained minimal. Ecotone analysis showed strong variability in transitional habitat edges, with peaks corresponding to increases in area-averaged risk indices. Territorial risk indices increased over time in all sites, reaching 0.470 in Gafsa (2012), 0.619 in Kairouan, and 0.507 in Sidi Bouzid (2020). These results indicate that irrigation-driven landscape changes enhance human – vector contact and transmission potential, underscoring the need to integrate irrigation practices into targeted, evidence-based vector management strategies.

ARTICLE HISTORY
Received 29 September 2025
Accepted 25 February 2026

KEYWORDS
Tunisia; leishmaniasis; semi-arid environments; landscape epidemiology, remote sensing

Introduction

Leishmaniasis in North Africa presents a complex and evolving epidemiological situation, shaped by several parasite species, mainly *Leishmania major*, *Leishmania tropica*, and *Leishmania infantum* (Aoun and Bouratbine 2014; Tabbabi 2019). Diverse phlebotomine sand fly vectors and multiple animal reservoirs contribute to sustained transmission cycles across different ecological contexts (Karmaoui et al. 2022). Historically, cutaneous leishmaniasis (CL), particularly zoonotic cutaneous leishmaniasis (ZCL) caused by *L. major*, has been the most widespread form in Morocco, Algeria, Tunisia, and Libya, with lower but notable incidence in Egypt (Aoun and Bouratbine 2014). In contrast, visceral leishmaniasis (VL) due to *L. infantum* remains endemic in specific foci and represents a severe, often fatal disease if untreated (Jain et al. 2023). For example, in Tunisia, zoonotic VL predominantly affects children and is associated with high in-hospital mortality, particularly among patients admitted late after symptom onset and presenting with bleeding, leukopenia, or hepatic cytolysis, highlighting the importance of early diagnosis and risk stratification (Ben Helel et al. 2017).

Each parasite species is associated with distinct transmission cycles. *Leishmania major* is zoonotic, with *Phlebotomus papatasi* as the principal vector and gerbils such as *Psammomys obesus* and jirds (*Meriones* spp.) as key reservoirs (Karmaoui et al. 2022). Laboratory studies demonstrate efficient transmission of *L. major* by *Ph. papatasi* to *Meriones shawi*, confirming this rodent as a competent reservoir. Infected hosts surviving the winter season can maintain parasite infectivity for several months, sustaining transmission between seasonal cycles (Derbali et al. 2012, 2014). Field studies in central Tunisia show that *Ph. papatasi* populations exhibit bimodal seasonal peaks in early spring and autumn, with lowest densities in midsummer. Notably, ZCL caused by *L. major* peaks several months after the autumn vector peak, particularly in Sidi Bouzid, demonstrating a close temporal link between vector abundance and human transmission (Chelbi et al. 2007).

CONTACT Attila J. Trájer trajer.attila@mk.uni-pannon.hu Sustainability Solutions Research Lab, University of Pannonia, Egyetem Utca 10, Veszprém H-8200, Hungary

Leishmania tropica may circulate in anthroponotic or zoonotic cycles depending on the settingand sand fly species (Tabbabi 2019). *Leishmania infantum* is responsible for both zoonotic visceral disease and cutaneous infections, with dogs as the major reservoirs (Aoun and Bouratbine 2014) and *Phlebotomus perniciosus* as the main vector in the Western Mediterranean basin (Slimane et al. 2014; Bouattour et al. 2021). This ecological diversity produces pronounced spatial heterogeneity in incidence, local outbreaks, and varied responses to control strategies (Tabbabi 2019). Recent entomological studies in central Tunisia document mixed transmission foci where ZCL caused by *L. major* and chronic cutaneous leishmaniasis associated with *L. tropica* cocirculate, involving diverse sand fly vectors. *Ph. papatasi* predominates in most biotopes, while *Ph. sergenti* dominates in mountainous areas, highlighting the risk of rural-to-urban spillover and the need for integrated vector control strategies (Abbas et al. 2022).

Temporal trends reveal both expansion and shifting endemicity. Since the 1980s, CL has expanded geographically in North Africa, with periodic epidemics reported, including peaks in the 1990s–2010s (Tabbabi 2019). Some foci declined after targeted interventions, while others have re-emerged or newly appeared, often at the margins of peri-urban or urban settlements (Benkhira et al. 2024). Population growth, urbanization, agricultural expansion, and inconsistent control efforts drive these patterns (Tabbabi 2019). Seasonality also strongly influences transmission. Sand fly populations, particularly *Ph. papatasi*, typically peak in summer (June – September), whereas human CL cases surge in autumn and winter (October – February), reflecting the incubation period and diagnostic delays (Karmaoui et al. 2022). Understanding these seasonal dynamics is critical for timing interventions such as insecticide spraying and reservoir management (Karmaoui et al. 2022).

Environmental and socio-economic drivers further complicate complexity. The climate itself plays a decisive role in the occurrence of phlebotomine vectors. For instance, field surveys in Tunisia have shown that *Ph. papatasi* is most abundant in arid and Saharan bioclimatic zones and rare in humid and subhumid regions, closely mirroring the spatial distribution of zoonotic cutaneous leishmaniasis caused by *L. major*. This strong ecological concordance underscores how climate- and environment-driven shifts in vector habitats shape regional disease risk (Chelbi et al. 2009). Climatic variability and long-term climate change alter vector ranges and season length (Tabbabi 2019). Land use changes, including irrigation and deforestation, reshape habitats for vectors and reservoirs (Aoun and Bouratbine 2014). Poverty, poor housing, and limited healthcare exacerbate disease burden (Jain et al. 2023), while human mobility and cross-border displacement facilitate parasite dispersal (Tabbabi 2019). Political instability and crises further weakensurveillance (Du et al. 2016). Spatiotemporal analyses in Sidi Bouzid reveal high-incidence clusters strongly associated with rural – urban gradients and major environmental modifications such as dam construction (Salah et al. 2007).

Surveillance across North Africa remains fragmented. WHO reports indicate Algeria, Morocco, and Tunisia rank among the highest-burden countries globally for CL (Jain et al. 2023). Underreporting complicates resource allocation and evaluation of control programs (Aoun and Bouratbine 2014). Public health responses include passive and active case detection, insecticide spraying, environmental sanitation, and reservoir management, and health education (Aoun and Bouratbine 2014). Nevertheless, challenges persist. Drugs are often toxic and expensive, require specialized infrastructure, and no widely available vaccine exists (Tabbabi 2019; Jain et al. 2023). Vector and reservoir control remains logistically complex (Aoun and Bouratbine 2014).

Tunisia exemplifies these challenges, with eco-epidemiology varying by clinical form due to distinct parasite – vector – reservoir systems shaped by climate, land use, and socio-economic conditions. Both CL and VL occur across heterogeneous ecological landscapes (Tabbabi 2019). ZCL due to *L. major* predominates in central and southern governorates such as Kairouan, Sidi Bouzid, and Gafsa, with recurrent autumn – winter outbreaks (Karmaoui et al. 2022). ACL caused by *L. tropica* occurs locally, while sporadic CL due to *L. infantum* reflects broader zoonotic transmission (Tabbabi 2019). VL persists in northern and central Tunisia, mainly affecting children (Aoun and Bouratbine 2014). Since the early 1980s, ZCL incidence has risen alongside ecological and agriculturalchanges, particularly irrigation, which expanded vector habitats (Aoun and Bouratbine 2014).

Irrigation and associated vegetation changes in central Tunisia create favorable microhabitats for Larroussius sand flies (*Phlebotomus perfiliewi*, *Ph. perniciosus*, *Ph. longicuspis*), important vectors of *L. infantum* (Fares et al. 2020). Surveys in Sidi Bouzid show *Ph. perfiliewi* is more abundant in irrigated

areas, with Larroussius species predominating over *Ph. papatasi*, supporting vector expansion (Barhoumi et al. 2015). These ecological changes facilitate stable *L. infantum* transmission. Studies in irrigated villages such as Saddaguia detected *L. infantum* DNA in multiple Larroussius species, providing an entomological basis for zoonotic VL emergence beyond historically endemic northern regions (Barhoumi et al. 2016). While long-term human incidence data by irrigation gradient are limited, evidence suggests transmission has expanded into central and southern arid regions alongside irrigation. In contrast, ZCL caused by *L. major* remains endemic in arid zones, with trends influenced by multiple ecological and control factors (World Health Organization, Regional Office for the Eastern Mediterranean 2025). Despite advances in research and control, operational constraints, reservoir resilience, and costly treatments sustain a high burden (Jain et al. 2023). Existing surveillance relies heavily on clinical case reporting, underestimating the true burden and failing to capture fine-scale ecological drivers of risk (Jain et al. 2023). Few studies have integrated remote sensing, machine learning, and landscape metrics to quantify habitat transitions, ecotone dynamics, and temporal relationship with disease risk (Dezfooli et al. 2025).

Addressing these gaps is essential for developing predictive tools and geographically targeted interventions that balance agricultural development with vector control in Tunisia and other arid and semi-arid regions.

Materials and methods

To assess the spatial risk of leishmaniasis in Tunisian urban and peri-urban settings, a geospatial classification and risk-indexing framework based on remote sensing imagery and supervised machine learning was developed. The methodological approach integrates spectral image analysis, ecological reasoning about vector habitats, and spatial risk modelling to capture the fine-scale environmental heterogeneity relevant to *Phlebotomus* sand fly populations and leishmaniasis transmission (Barhoumi et al. 2015, 2016).

Study sites

The study sites – Gafsa, Kairouan, and Sidi Bouzid – are located in central Tunisia and share an arid (Gafsa, Sidi Bouzid), and dry sub-humid (Kairouan) climates (Figure 1). These regions are characterized by relatively low and highly variable annual precipitation, high evapotranspiration rates, and pronounced seasonal temperature fluctuations, with hot summers and mild winters. The landscape is a mosaic of sparsely vegetated plains, irrigated agricultural fields, and semi-natural habitats, providing a heterogeneous environment that influences *Phlebotomus* sand fly distribution and leishmaniasis transmission risk (Chelbi et al. 2022). The combination of climatic stress and anthropogenic landscape modifications, such as irrigation and urban expansion, makes these central Tunisian regions particularly relevant for studying environmental drivers of leishmaniasis (Aoun and Bouratbine 2014).

Satellite image data source

High-resolution RGB satellite images were obtained from Google Earth (Google LLC; Gorelick 2013) for 1984–2020; for Kairouan the series begins in 1985, as the 1984 image was obscured by cloud cover. Google Earth imagery integrates orthorectified and mosaicked data from multiple sensors and providers, including Landsat (NASA/USGS), Sentinel (ESA), SPOT, and commercial high-resolution satellites, with spatial resolutions ranging from 30 m (Landsat archive) to sub-meter (recent commercial sources). RGB composites based on the visible spectrum allow detection of vegetation cover, water bodies, soil exposure, and anthropogenic land-use features – key proxies for vector habitats and reservoir host distribution. To ensure temporal consistency, only December images were used, as vegetation is typically senescent, reducing seasonal greenness variability, and imagery is generally clearer and less cloud-affected than in wetter months.

Delaminating coordinates of the studied grids were as follows: 34.35–34.50 N, 8.63–8.94 E (Gafsa), 9.84–10.32 E, 35.56–35.79 N (Kairouan), and 34.98–35.13 N, 9.22–9.54 E (Sidi Bouzid). The selected grids cover both the city regions in the strict sense and their narrower environments.

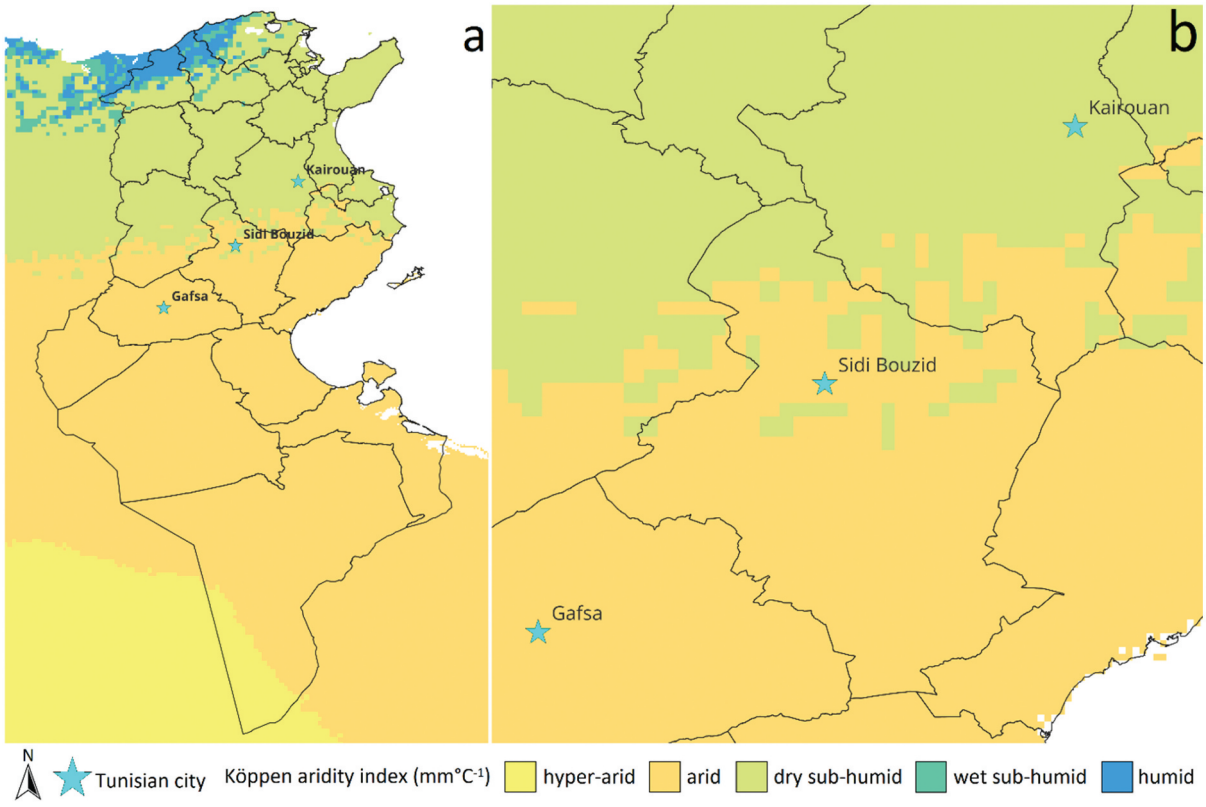

Figure 1. The studied sites in central Tunisia projected to the Köppen aridity index map of Tunisia (a) and central Tunisia (b) based on the classification of Quan et al. (2013, 2014).

Data preprocessing and feature extraction

RGB data were transformed into numerical descriptors by extracting spectral band values (red, green, blue) and perceptual features from the HSL colour space (hue, saturation, lightness). Integrating RGB and HSL parameters allowed for the detection of vegetation vigour, soil brightness, and anthropogenic surface contrasts – key environmental factors shaping sand fly ecology and reservoir host distribution in arid and semi-arid settings (Barhoumi et al. 2015; Tabbabi et al., 2019).

While multispectral and infrared imagery are widely applied in disease ecology, RGB data offer distinct advantages in terms of accessibility, reproducibility, and temporal depth. For example, Google Earth provides global RGB archives dating back to the mid-1980s, enabling consistent monitoring of land-use change, vegetation dynamics, and habitat modification relevant to *Leishmania* risk without the need for specialized processing (Potere 2008; Yu and Gong 2012).

Furthermore, RGB imagery is intuitive to interpret across disciplines, supporting interdisciplinary applications in public health and environmental management (Goodchild 2007). This accessibility not only enhances reproducibility but also facilitates broader participation, making the method well-suited for citizen science initiatives.

Supervised classification

An annotated training dataset was compiled from field-validated samples stored in an Excel table, in which each pixel was associated with a categorical status representing environmental suitability classes. A Random Forest classifier with 200 decision trees was trained on this dataset, with a 70/30 train – test split to ensure robust performance assessment. Model accuracy was evaluated using the hold-out test set, yielding an accuracy metric that quantified the reliability of the classifier in discriminating habitat-related surface categories. Random Forests were chosen due to their high performance on non-linear classification

problems and their capacity to handle multi-dimensional spectral inputs, which is particularly useful for heterogeneous urban – agricultural mosaics (Cutler et al. 2007).

Spatial prediction and habitat mapping

The trained classifier was then applied to the entire satellite image. Each pixel was assigned to one of the previously defined categories, producing a categorical habitat map of the city and its narrower environment, including the peri-urban regions. This step allowed the identification of potential sand fly habitats and ecotones at fine spatial resolution. The approach follows similar applications of remote sensing in North African leishmaniasis studies, where land-cover classes have been linked to *Phlebotomus* abundance and parasite circulation (Barhoumi et al. 2015; Benkhira et al. 2024).

Ecotone analysis

Edge-rich mosaics are recognized as risk-enhancing environments, as transitional zones can favour sand fly breeding and host – vector contact (Alexander and Maroli 2003; Barhoumi et al. 2016). Ecotones – boundaries between habitat categories – were systematically quantified by analysing neighbouring pixel relationships. This was performed by iterating over all pixel pairs and identifying transitions between categories. The relative length of ecotones, expressed as the number of boundary pixels, was used as an ecological indicator.

Risk index calculation and justification of weights

To convert categorical classifications into epidemiological risk, baseline weights were assigned to habitat classes. The applied weights were as follows: dry/urbanized habitats: 0.2 (Ben-Ismail et al. 1987; Orshan et al. 2016); irrigated/peri-irrigated habitats: 0.7 (Barhoumi et al. 2015, 2016); semi-natural habitats, primarily or secondarily arid, semi-arid steppes: 0.5 (Tabbabi et al. 2011); and 0 for bare rock surface areas without any vegetation, reflecting their relative suitability for *Phlebotomus* vectors and *Leishmania* transmission.

Category 1 (0.7) represents irrigated and peri-irrigated habitats, consistently linked to high densities of *Ph. perfiliewi* and *Ph. perniciosus* and elevated *L. infantum* infection rates in central Tunisia (Barhoumi et al. 2015, 2016). Category 2 (0.5) corresponds to semi-natural habitats, which support moderate sand fly abundance and variable infection potential depending on vegetation, hosts, and soil conditions (Tabbabi et al. 2011; Barhoumi et al. 2015). Category 0 (0.2) denotes dry or urbanized zones, generally unsuitable for breeding, though *Ph. papatasi* may persist in xeric habitats with rodent burrows; overall risk remains low (Ben-Ismail et al. 1987; Orshan et al. 2016).

To capture the epidemiological role of habitat edges, ecotone "bonus" values (0.1, 0.2, and 0.3 for 0–1, 1–2, and 0–2 pairs) were added, with higher values reflecting sharper ecological contrasts. Such transitions often enhance sand fly abundance and human – vector contact (Alexander and Maroli 2003; Ready 2013; Barhoumi et al. 2016).

The resulting risk index integrates intrinsic habitat suitability with ecotone effects, consistent with landscape epidemiology frameworks that emphasize the disproportionate role of habitat edges and heterogeneous mosaics in vector-borne disease transmission (Ready 2013; Shirzadi et al. 2020). Table 1 able 1 summarizes the correspondence between classified land-cover clusters, dominant land surface types, and habitat-based risk categories, and presents the baseline risk weights and ecotone bonus values applied in the risk index calculation.

Table 1. Habitat classes, corresponding land-cover clusters, baseline risk weights, and ecotone bonuses used for leishmaniasis risk index calculation.

Habitat class	Corresponding cluster	Dominant land surface type	Baseline risk	Bonus with 0	Bonus with 1	Bonus with 2
0	Cluster 1	Dry/urbanized, sparsely vegetated	0.2	–	0.1	0.3
1	Cluster 2	Irrigated/vegetated, peri-urban	0.7	0.1	–	0.2
2	Cluster 3	Semi-natural/mixed land cover	0.5	0.3	0.2	–
–	Cluster 4	Bare, marginal, or highly disturbed	0	–	–	–

The baseline habitat weights used in the risk index were derived from published ecological and epidemiological studies and therefore reflect empirically constrained suitability classes rather than free model parameters. While alternative weighting schemes may shift absolute index values, the relative spatial patterns and temporal trends are primarily driven by land-cover composition and ecotone structure. Consequently, the comparative interpretation of risk dynamics among cities and across years is expected to be robust to moderate variations in individual weight assignments.

Software and statistics

All data processing, image analysis, and modelling steps were implemented in the Python 3.10 (64-bit) programming environment using open-source scientific libraries. Supervised classification was performed using a Random Forest algorithm, and pixel-wise risk indices were calculated by integrating baseline habitat suitability values with neighbourhood-based ecotone bonuses and texture-derived modifiers.

While neighbouring pixels in remotely sensed imagery are inherently spatially autocorrelated (Goodchild 2007), the analytical objective of this study was not statistical inference at the pixel level. Spatial autocorrelation is primarily problematic for regression-based inference when individual observations are assumed to be independent, whereas it is not a limitation for descriptive, exploratory, or pattern-oriented spatial analyses (Dormann et al. 2007). In the present study, spatial dependence was therefore treated as an inherent characteristic of the landscape and as meaningful ecological information rather than as a statistical bias.

Analyses focused on identifying and comparing spatially structured environmental patterns relevant to sand fly ecology and leishmaniasis transmission (Waitz et al. 2019), including land-cover composition, habitat mosaics, and ecotone development. Neighbourhood relationships were incorporated through median filtering, ecotone detection, and local risk bonuses to capture edge effects and habitat continuity influencing *Phlebotomus* distribution and human – vector contact. Risk indices were summarized using mean, minimum, maximum, and standard deviation values to describe relative spatial patterns and temporal trends. Spatial autocorrelation was treated as an intrinsic ecological signal rather than a violation of model assumptions.

The leishmaniasis risk-assessed images can be accessed via Zenodo (DOI: 10.5281/zenodo.17175199).

Results

Gafsa

The spatial and temporal analysis of land-cover clusters in Gafsa between 1984 and 2020 revealed dynamic patterns in habitat composition relevant to leishmaniasis risk. Across the study period, Cluster 1, representing low-risk or sparsely vegetated areas, consistently occupied the largest relative area, ranging from 49.2% in 2011 to 68.3% in 2001, with a mean value of approximately 61.3%. Cluster 2, corresponding to habitats with high ecological suitability for *Phlebotomus* sand flies (primarily irrigated or peri-irrigated areas), exhibited relative areas between 11.7% (1988) and 21.4% (2018), reflecting gradual expansion in certain years, particularly after the mid-1990s. Cluster 3, representing intermediate-risk or semi-natural habitats, ranged from 15.5% (2001) to 31.3% (2012), indicating temporal fluctuations linked to environmental and anthropogenic changes. The relative area of Cluster 4 remained minimal (<2.5%) throughout the period, suggesting marginal contribution to overall leishmaniasis risk. The combined standard deviation of Clusters 1–3 relative areas was 10.3–15.2%, indicating moderate interannual variability (Figure 2).

Ecotone analysis demonstrated substantial spatial interactions between habitat categories. The boundary length between Clusters 1 and 3 ranged from 44,277 pixels (1985) to 114,645 pixels (2008), highlighting significant variation in the extent of transitional zones across years. Ecotone lengths between Clusters 1 and 2 and between Clusters 2 and 3 also displayed considerable interannual variability, with particularly high values observed in 2001 for the 0–1 pair (118,578 pixels) and in 2010 for the 1–2 pair (100,975 pixels). These results underscore the temporal dynamics of habitat mosaics, which likely influence vector movement and human – vector contact probabilities. The standard deviation of ecotone lengths across all pairwise

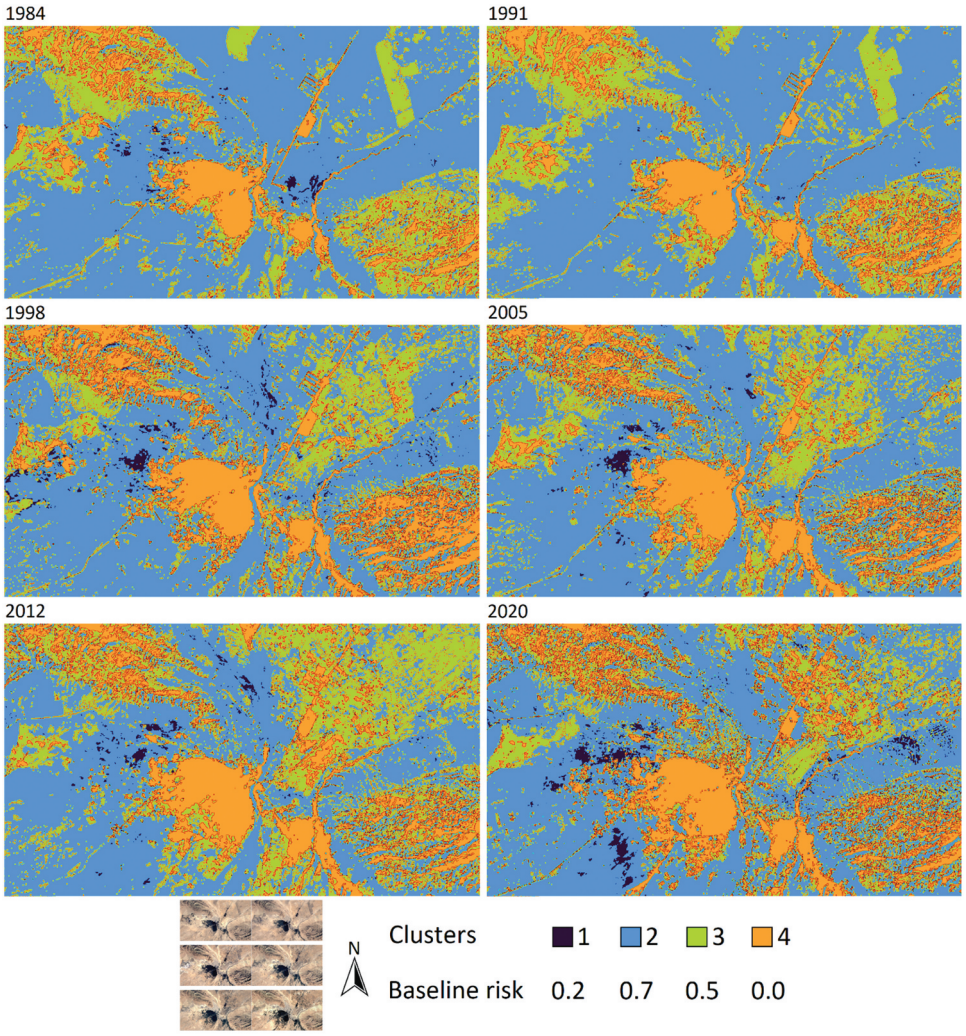

Figure 2. Habitat clusters and associated leishmaniasis risk in Gafsa, central Tunisia in different example years. Clusters are defined as follows: cluster 1—sparsely vegetated areas with low vector suitability; cluster 2—irrigated or peri-urban habitats with high leishmaniasis risk; cluster 3—semi-natural or partially irrigated habitats with moderate suitability; cluster 4—marginal or highly disturbed habitats (<1%). Clusters are coloured according to their associated baseline leishmaniasis risk values (see legend and Table 1); final risk surfaces additionally incorporate ecotone-based bonuses. Inset: original RGB satellite images of Gafsa corresponding to the processed cluster map above.

combinations of Clusters 1–3 ranged from approximately 22,500 to 48,200 pixels, reflecting both gradual trends and episodic peaks in habitat heterogeneity (Figure 3).

Kairouan

The analysis of habitat clusters in Kairouan from 1984 to 2020 revealed notable temporal and spatial variations in land-cover composition, with implications for leishmaniasis risk. Cluster 1, representing low-risk or sparsely vegetated areas, showed substantial interannual variability, ranging from 20.1% in 2012 to 47.9% in 2000. Cluster 2, corresponding to highly suitable habitats for *Phlebotomus* sand flies (primarily irrigated or peri-irrigated areas), fluctuated between 11.7% (1995) and 33.1% (2017), with increases in the late 1990s and mid-2000s reflecting anthropogenic landscape modifications. Cluster 3, representing intermediate-risk semi-natural habitats, accounted for the largest proportion of the landscape in most years, ranging from 35.1% (2016) to 57.4% (1996), indicating that a significant portion of the environment remains conducive to vector presence. Cluster 4 remained minimal throughout the period (<0.8%), suggesting a negligible contribution to overall leishmaniasis risk. The standard deviation of relative areas

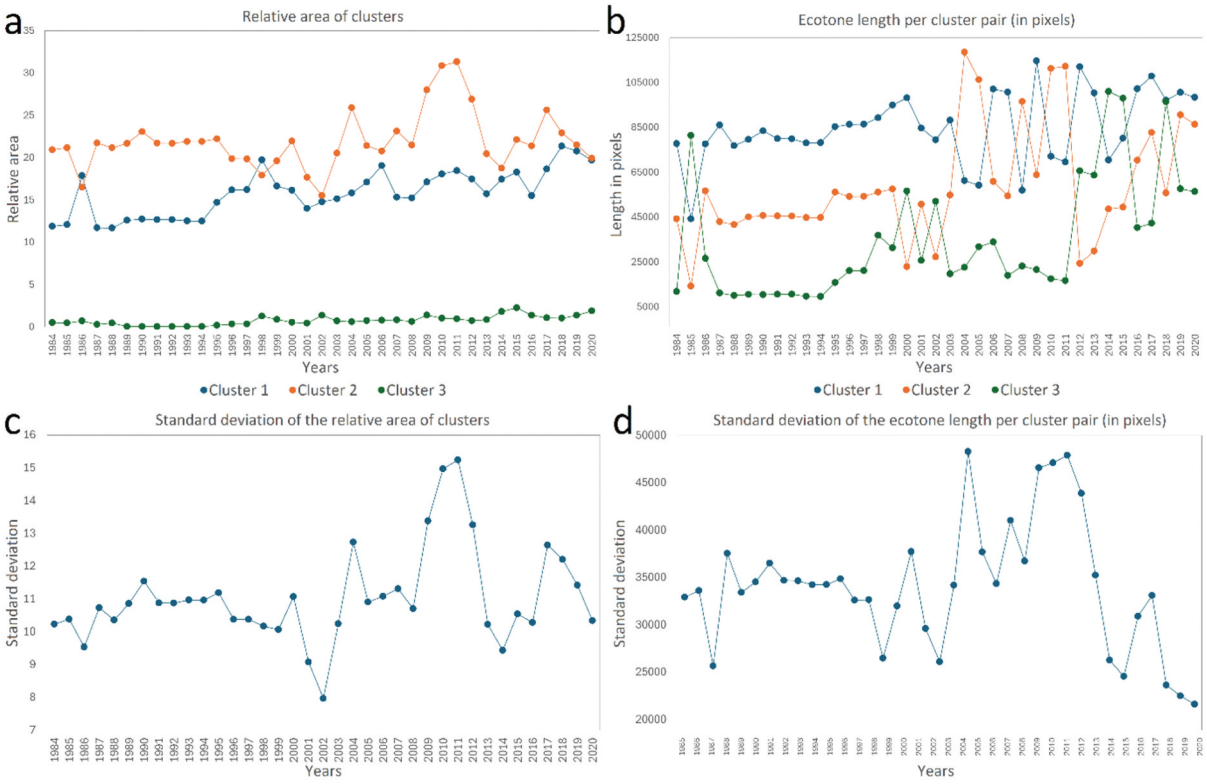

Figure 3. Statistics of the relative change of land cover clusters in Gafsa. a: relative area of clusters; b: ecotone length per cluster pair; c: standard deviation of cluster areas; d: standard deviation of ecotone lengths.

for Clusters 1–3 ranged from approximately 4.8% to 25.8%, indicating high interannual variability and heterogeneous landscape dynamics (Figure 4).

Ecotone analysis demonstrated pronounced variability in the extent of habitat edges. The boundary length between Clusters 1 and 3 varied from 110,595 pixels (2004) to 177,304 pixels (2012), illustrating temporal shifts in transitional zones. Ecotone lengths between Clusters 1 and 2 and between Clusters 2 and 3 also exhibited substantial fluctuations, with exceptionally high values in 2015 for the 1–2 pair (143,806 pixels) and in 2016 for the 2–3 pair (164,515 pixels). These observations suggest that transitional habitats, which favour sand fly movement and human – vector contact, were particularly dynamic over the study period. The standard deviation of ecotone lengths for Clusters 1–3 ranged from approximately 58,500 to 74,000 pixels, reflecting both gradual trends and episodic peaks in habitat heterogeneity (Figure 5).

Sidi Bouzid

The temporal analysis of habitat clusters in Sidi Bouzid from 1984 to 2020 revealed dynamic patterns of landscape composition relevant to leishmaniasis risk. Cluster 1, representing low-risk or sparsely vegetated areas, exhibited substantial interannual variability, ranging from 28.7% in 2012 to 53.4% in 1988. Cluster 2, corresponding to highly suitable habitats for *Phlebotomus* sand flies, including irrigated or peri-irrigated areas, showed an increasing trend over the study period, ranging from 9.7% in 1984 to 34.1% in 2020, indicating progressive landscape modifications favourable for vector proliferation. Cluster 3, representing intermediate-risk semi-natural habitats, remained a major component of the landscape, varying between 29.8% in 2016 and 48.1% in 1990. Cluster 4 remained minimal (<0.6%) throughout the study period, suggesting negligible contribution to overall risk. The standard deviation of Clusters 1–3 relative areas ranged from approximately 1.1% to 21.6%, reflecting moderate to high interannual landscape variability (Figure 6).

Ecotone analysis indicated substantial temporal variation in habitat edge length, which is a key factor in *Phlebotomus* movement and human – vector interactions. The boundary length between Clusters 1 and 3

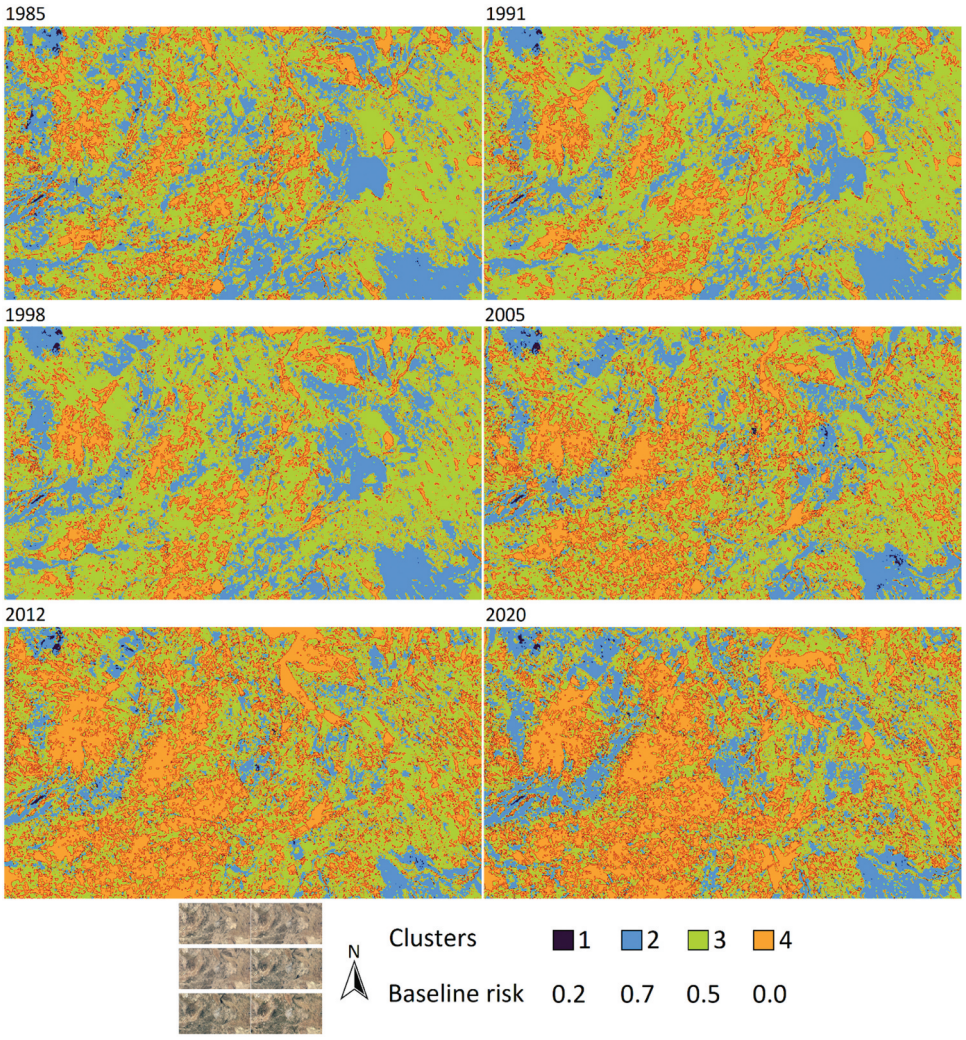

Figure 4. Habitat clusters and associated leishmaniasis risk in Kairouan, central Tunisia in different example years (cluster definitions as in Fig. 2). Clusters are coloured according to their associated baseline leishmaniasis risk values (see legend and Table 1); final risk surfaces additionally incorporate ecotone-based bonuses. Inset: original RGB satellite images of Kairouan corresponding to the processed cluster map above.

varied from 30,390 pixels in 2011 to 171,758 pixels in 2017, highlighting significant fluctuations in transitional habitats. Ecotone lengths between Clusters 1 and 2 and between Clusters 2 and 3 also showed considerable interannual variation, with peaks observed in 1995 for the 1–2 pair (112,371 pixels) and in 2016 for the 2–3 pair (107,551 pixels). The standard deviation of ecotone lengths across all pairwise cluster combinations ranged from approximately 45,300 to 62,100 pixels, demonstrating both gradual trends and episodic peaks in habitat heterogeneity (Figure 7).

Risk index trends

Across all sites, the area-averaged leishmaniasis risk index increased over the study period, tracking irrigation expansion and ecotone development. In Gafsa, values rose from 0.377 (1988) to 0.470 (2012), with stable levels (~0.38–0.39) in early years, followed by growth from the mid-1990s onward. In Kairouan, risk was consistently higher, ranging from 0.507 (1994) to 0.619 (2012), with early values already moderate (0.511–0.542), then rising sharply in the 2000s. Sidi Bouzid showed a steady increase, from 0.450 (1988) to 0.592 (2020), with sustained high risk in the 2000s–2010s. Peaks in all regions coincided with periods of extensive ecotones, confirming that transitional habitats amplify vector – human contact and transmission potential (Figure 8).

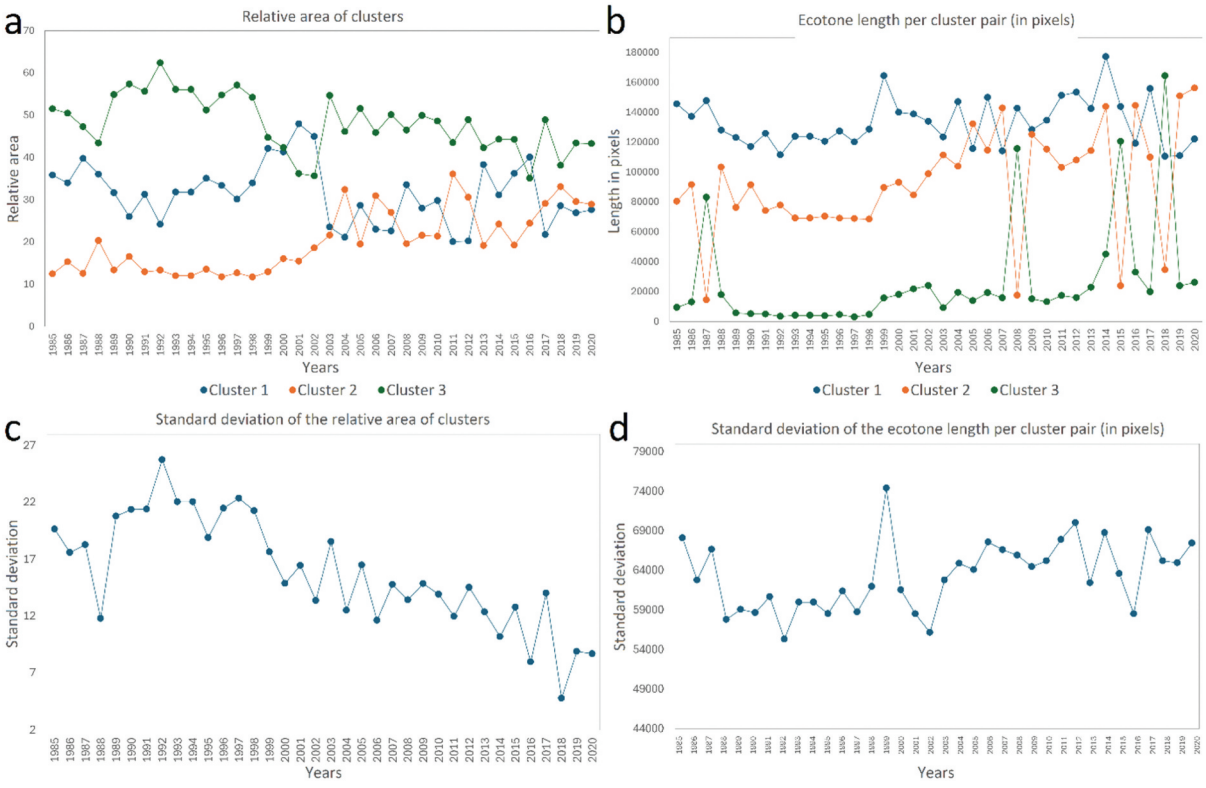

Figure 5. Statistics of the relative change of land cover clusters in Kairouan. Same variables and panel structure as Figure 3.

Linear regression analyses revealed increasing territorial risk across all three cities over the study period. Gafsa exhibited a strong upward trend, indicating a consistent rise in risk, while Kairouan showed a moderate increase. Sidi Bouzid displayed the most pronounced escalation, suggesting a rapid intensification of territorial risk compared to the other two cities. These patterns highlight spatial variability in risk dynamics, with Sidi Bouzid representing the most critical area for surveillance and targeted interventions (see Table 2 for detailed regression statistics).

Discussion

The Tunisian case illustrates how environmental modification, especially irrigation, fundamentally reshapes leishmaniasis epidemiology. Entomological studies demonstrate that irrigation projects in central Tunisia create favourable microhabitats for Larroussius sand flies, the vectors of *L. infantum*. Species such as *Phlebotomus perfiliewi* and *Ph. perniciosus* reach higher densities in irrigated areas than in dry zones, directly linking irrigation to elevated VL risk (Barhoumi et al. 2015, 2016). Earlier research also noted that irrigation-driven habitat changes favoured Larroussius species at the expense of xerophilic species, reshaping local epidemiology (Barhoumi et al. 2012). In contrast, *Ph. papatasi*, the main *L. major* vector, thrives in dry, rodent-rich habitats. Expansion of irrigation reduces its dominance while facilitating Larroussiusproliferation, shifting disease risk from CL toward VL (Orshan et al. 2016). This entomological transition is mirrored by epidemiological data from central Tunisia, where the growth of irrigated and peri-irrigated landscapes coincides with increasing VL incidence and the emergence of new endemic foci, while zoonotic CL becomes relatively less dominant (Barhoumi et al. 2016). Field investigations further confirm that *Ph. perfiliewi* is significantly more abundant in irrigated areas of southern Tunisia, implicating irrigation expansion in altered vector ecology and disease risk (Barhoumi et al. 2015).

Reservoir dynamics reinforce these patterns. The abundance of rodents, including *Meriones* spp. and *Psammomys obesus*, responds positively to vegetation and habitat changes driven by irrigation, as observed in Tunisia (Ettiss et al. 2020). Dogs, the principal reservoirs of *L. infantum*, are increasingly exposed to dense sand fly populations in irrigated villages, strengthening zoonotic VL cycles (Derghal et al. 2022).

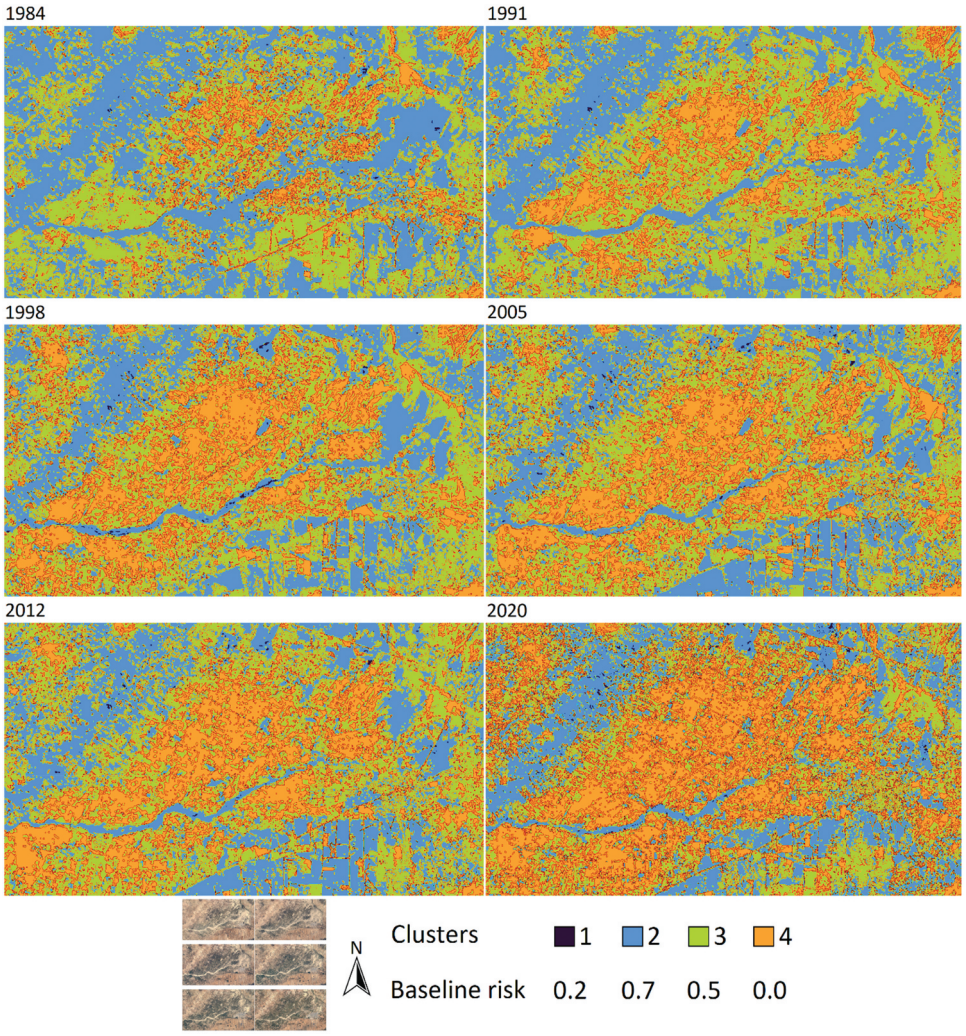

Figure 6. Habitat clusters and associated leishmaniasis risk in Sidi Bouzid, central Tunisia in different example years (cluster definitions as in Fig. 2). Clusters are coloured according to their associated baseline leishmaniasis risk values (see legend and Table 1); final risk surfaces additionally incorporate ecotone-based bonuses. Inset: original RGB satellite images of Sidi Bouzid corresponding to the processed cluster map above.

Therefore, irrigation not only modifies vector ecology but also enhances reservoir exposure, intensifying transmission potential. Spatiotemporal analysis of Gafsa, Kairouan, and Sidi Bouzid between 1984 (1985) and 2020 confirmed these dynamics. Irrigated and peri-irrigated habitats (Cluster 2) consistently exhibited the highest suitability for sand fly presence and expanded markedly from the mid-1990s onward (Chemak et al. 2022). Analysis of ecotones – habitat boundaries between clusters – revealed that transitional zones amplified potential human – vector contact. Peaks in ecotone length coincided with elevated risk indices, consistent with prior findings that transitional habitats as hotspots of transmission (Mili et al. 2012; Aoun and Bouratbine 2014).

Regional patterns further highlight the link between anthropogenic change and disease dynamics. In Gafsa, VL risk rose moderately but steadily, whereas in Kairouan and Sidi Bouzid, increases were sharper, particularly in the 2000s–2010s. These trends parallel irrigation expansion and peri-urban growth, both of which favour sand fly proliferation (Barhoumi et al. 2015, 2016). The minimal contribution of highly unsuitable habitats (Cluster 4) underscores the tight dependence of sand fly presence on microenvironmental conditions (Ready 2013). Collectively, these findings demonstrate that both habitat composition and edge dynamics shape transmission risk. Management strategies should therefore target not only high-suitability irrigated habitats but also transitional zones where human – vector contact intensifies. Furthermore, the temporal evolution of risk emphasizes the importance of continuous monitoring, as landscape and social changes drive

Figure 7. Statistics of the relative change of land cover clusters in Sidi Bouzid. Same variables and panel structure as Figure 3.

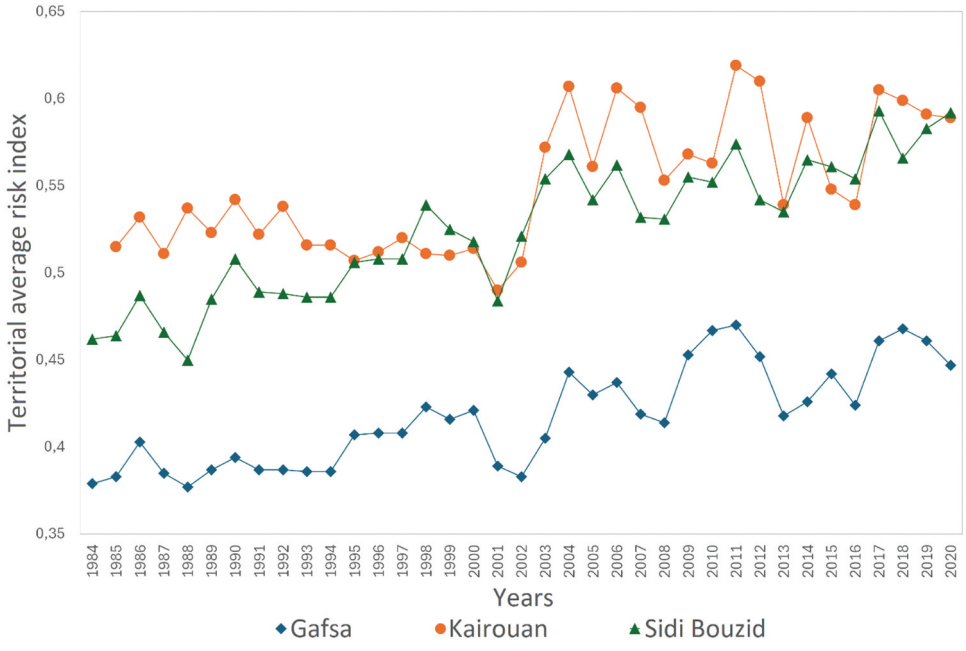

Figure 8. The changes of the territorial average risk index for leishmaniasis in three central Tunisian cities in 1984–2020.

shifting endemicity. Integrating remote sensing, landscape metrics, and machine learning provides a robust framework for predicting leishmaniasis risk (Dezfooli et al. 2025). At the same time, ecological evidence shows that irrigation contributes to socioeconomic resilience while unintentionally creating conditions favourable to Larroussius vectors and VL transmission (Barhoumi et al. 2015). Balancing agricultural development with

Table 2. Results of linear regression analyses by city.

City	N	Slope	R^2	p-value	95% CI slope
Gafsa	37	0.00224	0.70	<.0001	0.0017–0.0027
Kairouan	36	0.00244	0.46	<.0001	0.0015–0.0034
Sidi Bouzid	37	0.00331	0.83	<.0001	0.0028–0.0038

vector management requires integrated One Health strategies that explicitly incorporate irrigation practices into disease prevention (World Health Organization 2023; Kalitsilo et al. 2025).

Beyond central Tunisia, these findings are relevant to other semi-arid regions experiencing rapid agricultural and hydrological transformation, particularly across the Maghreb and the Middle East. Drought threatens agroforestry landscapes and dryland livelihoods in North Africa, where environmental change is particularly pronounced (Kmoch et al. 2024). Similar irrigation-driven landscape changes have been documented in Algeria, Morocco, Libya, and parts of the Middle East. Expansion of irrigated perimeters and peri-urban agriculture alters soil moisture, vegetation cover, and microclimatic conditions (Benabdelkader et al. 2021; Al Hamedi et al. 2023; Haddad et al. 2023). These environmental modifications favor Larroussius sand flies, including *Ph. perniciosus* and *Ph. perfiliewi*, which are also established vectors of *L. infantum* throughout the Mediterranean basin (Calzolari et al. 2022; Chelbi et al. 2022; Jarallah et al. 2022; Olmeda et al. 2024). Consequently, irrigation may similarly shift local transmission systems from predominantly zoonotic CL toward VL in these regions.

The importance of ecotones as zones of amplified human – vector contact is likewise transferable to other semi-arid landscapes characterized by fragmented land use, such as irrigated fields adjacent to settlements, rangelands, wadis, and oasis-desert boundaries (Barhoumi et al. 2021; Karmaoui et al. 2023). In many Maghreb and Middle Eastern settings, these transitional habitats coincide with increased human activity and domestic animal presence, potentially intensifying exposure to infected vectors (Tabbabi 2019; Baaziz et al. 2024). Furthermore, reservoir dynamics involving dogs and rodents that respond to vegetation change appear consistent across these regions, suggesting that irrigation-driven ecological cascades operate through similar vector – reservoir – human interfaces (Ghatee et al. 2023).

While local ecological, socioeconomic, and climatic conditions modulate specific outcomes, the Tunisian case illustrates a generalizable mechanism by which anthropogenic water management reshapes leishmaniasis risk in semi-arid environments. Integrating irrigation planning with vector surveillance, landscape monitoring, and One Health – oriented interventions – a strategy promoted by the World Health Organization (World Health Organization, UNEP United Nations Environment Programme, & World Organisation for Animal Health 2022) – may therefore be broadly applicable across semi-arid regions facing comparable development trajectories (Shadomy et al. 2025). Risk mapping approaches developed for Tunisia may inform surveillance and intervention strategies elsewhere, particularly in regions experiencing irrigation-driven landscape transformations.

In conclusion, the interplay between irrigation, habitat heterogeneity, and vector – reservoir ecology explains the persistence and intensification of leishmaniasis risk in central Tunisia. Future priorities should include geographically targeted surveillance, ecological modelling, and integrated vector management adapted to anthropogenic landscapes.

Disclosure statement

No potential conflict of interest was reported by the author.

Funding

This paper was supported by the János Bolyai Research Scholarship of the Hungarian Academy of Sciences under grant number: bo/00896/24/5.

ORCID

Attila J. Trájer http://orcid.org/0000-0003-3248-6474

Biographical note

Attila J. Trájer is a Hungarian physician and researcher specializing in environmental health, epidemiology, and the ecology of vector-borne and parasitic diseases. His work integrates medical sciences with climatology, landscape ecology, and geoinformatics, with a particular focus on how climate change and environmental transformations shape the distribution of infectious diseases. He has published extensively on leishmaniasis, malaria, and other parasitic infections, combining field ecology, modeling approaches, and historical perspectives.

CRediT roles AJT

Conceptualization, Data curation, Formal analysis, Funding acquisition, Investigation, Methodology, Project administration, Resources, Software, Supervision, Validation, Visualization, Roles/Writing – original draft, and Writing – review & editing.

Data availability statement

The leishmaniasis risk-assessed images can be accessed via Zenodo (DOI: 10.5281/zenodo.17175199).

References

Abbas MAS et al. 2022. Independent circulation of *Leishmania major* and *Leishmania tropica* in their respective sandfly vectors for transmission of zoonotic and chronic cutaneous leishmaniasis co-existing in a mixed focus of central Tunisia. Pathogens. 11(8):855. https://doi.org/10.3390/pathogens11080855

Alexander B, Maroli M. 2003. Control of phlebotomine sandflies. Med Vet Entomol. 17(1):1–18. https://doi.org/10.1046/j.1365-2915.2003.00407.x

Al Hamedi FH et al. 2023. Wastewater irrigation: a promising way for future sustainable agriculture and food security in the United Arab Emirates. Water. 15(12):2284. https://doi.org/10.3390/w15122284

Aoun K, Bouratbine A. 2014. Cutaneous leishmaniasis in North Africa: a review. Parasite. 21(2014):14. https://doi.org/10.1051/parasite/2014014

Baaziz S, Sadeddine R, Zeroual F, Benakhla A, Righi S. 2024. Canine leishmaniasis in Maghreb countries: a systematic review and meta-analysis. J Vector Borne Dis. 61(4):515–524. https://doi.org/10.4103/JVBD.jvbd_2_24

Barhoumi W et al. 2015. Irrigation in the arid regions of Tunisia impacts the abundance and apparent density of sand fly vectors of *Leishmania infantum*. Acta Trop. 141(2015):73–78. https://doi.org/10.1016/j.actatropica.2014.10.008

Barhoumi W et al. 2016. Changes of sand fly populations and *Leishmania infantum* infection rates in an irrigated village located in arid central Tunisia. Int J Environ Res Public Health. 13(3):329. https://doi.org/10.3390/ijerph13030329

Barhoumi W et al. 2021. Risk assessment of the role of the ecotones in the transmission of zoonotic cutaneous leishmaniasis in central Tunisia. Int J Environ Res Public Health. 18(17):9274. https://doi.org/10.3390/ijerph18179274

Barhoumi W, Chelb I, Zhioua E. 2012. Effet du développement des systèmes d'irrigation dans les zones arides sur l'établissement de *Phlebotomus* (*Larroussius*) *perfiliewi* Parrot, 1939. Bull Soc Pathol Exot. 105(5):403–405. https://doi.org/10.1007/s13149-012-0261-x

Benabdelkader M, Saifi R, Saifi H. 2021. Sustainable agriculture in some Arab Maghreb countries (Morocco, Algeria, Tunisia). In: Abu-Hashim M, Khebour Allouche F, Negm A, editors. Agro-environmental sustainability in MENA regions. Springer Water. Springer. pp. 233–261.https://doi.org/10.1007/978-3-030-78574-1_10

Ben Helel K et al. 2017. Risk factors for mortality of children with zoonotic visceral leishmaniasis in central Tunisia. PLOS ONE. 12(12):e0189725. https://doi.org/10.1371/journal.pone.0189725

Ben-Ismail R, Gramiccia M, Gradoni L, Helal H, Ben Rachid MS R. Soc, editor. 1987. Isolation of *Leishmania major* from *Phlebotomus papatasi* in Tunisia. Trop Med Hyg. 81(5):749–750. https://doi.org/10.1016/0035-9203(87)90018-6

Benkhira S, Boudebouch N, Benazzouz B. 2024. The spatio-temporal evolution of leishmaniasis in the province of Essaouira. Front Epidemiol. 4(2024):1462271. https://doi.org/10.3389/fepid.2024.1462271

Bouattour A et al. 2021. Canine leishmaniosis in Tunisia: growing prevalence, larger zones of infection. PLOS Negl Trop Dis. 15(12):e0009990. https://doi.org/10.1371/journal.pntd.0009990

Calzolari M et al. 2022. Host preference and *Leishmania infantum* natural infection of the sand fly *Phlebotomus perfiliewi* in northern Italy. Acta Trop. 226:106246. https://doi.org/10.1016/j.actatropica.2021.106246

Chelbi I et al. 2007. Phenology of *Phlebotomus papatasi* (Diptera: psychodidae) relative to the seasonal prevalence of zoonotic cutaneous leishmaniasis in central Tunisia. J Med Entomol. 44(2):385–388. https://doi.org/10.1093/jmedent/44.2.385

Chelbi I et al. 2022. Investigation of the sandfly fauna of central arid areas and northern humid regions of Tunisia, with morphological and molecular identification of the Recently established population of *Phlebotomus* (*Larroussius*) *perfiliewi*. Insects. 13(11):1057. https://doi.org/10.3390/insects13111057

Chelbi I, Kaabi B, Bejaoui M, Derbali M, Zhioua E. 2009. Spatial correlation between *Phlebotomus papatasi* Scopoli (Diptera: psychodidae) and incidence of zoonotic cutaneous leishmaniasis in Tunisia. J Med Entomol. 46 (2):400–402. https://doi.org/10.1603/033.046.0229

Chemak F, Nouiri I, Bellali H, Chahed MK. 2022. Irrigation practices, prevalence of leishmaniasis and sustainable development: evidence from the Sidi Bouzid region in central Tunisia. Sci Afr. 15(2022):e01094. https://doi.org/10.1016/j.sciaf.2022.e01094

Cutler DR et al. 2007. Random forests for classification in ecology. Ecology. 88(11):2783–2792. https://doi.org/10.1890/07-0539.1

Derbali M et al. 2014. Laboratory and field evaluation of rodent bait treated with fipronil for feed through and systemic control of *Phlebotomus papatasi*. Acta Trop. 135(2014):27–32. https://doi.org/10.1016/j.actatropica.2014.03.013

Derbali M, Chelbi I, Ben Hadj Ahmed S, Zhioua E. 2012. *Leishmania major* Yakimoff et Schokhor, 1914 (Kinetoplastida: Trypanosomatidae) chez *Meriones shawi* Duvernoy, 1842 (Rodentia: Gerbillidae): persistance de l'infection du mérion et de son infectivité pour le phlébotome vecteur *Phlebotomus* (*Phlebotomus*) *papatasi* Scopoli, 1786 (Diptera: Psychodidae). Bull Soc Pathol Exot. 105(5):399–402. https://doi.org/10.1007/s13149-012-0259-4

Derghal M et al., S. (2022. High-resolution melting analysis identifies reservoir hosts of zoonotic *Leishmani*a parasites in Tunisia. Parasit Vectors. 15(1):12. https://doi.org/10.1186/s13071-021-05138-x

Dezfooli FP, Zoej MJV, Youssefi F, Ghaderpour E. 2025. Integrating remote sensing, GIS, and machine learning for zoonotic cutaneous leishmaniasis modelling. Environ Res Commun. 7(8):085017. https://doi.org/10.1088/2515-7620/adfbbe

Dormann CF et al. 2007. Methods to account for spatial autocorrelation in the analysis of species distributional data: a review. Ecography. 30(2007):609–628. https://doi.org/10.1111/j.2007.0906-7590.05171.x

Du R, Hotez PJ, Al-Salem WS, Acosta-Serrano A. 2016. Old world cutaneous leishmaniasis and refugee crises in the middle East and North Africa. PLOS Negl Trop Dis. 10(5):e0004545. https://doi.org/10.1371/journal.pntd.0004545

Ettiss K, Chammem M, Khorchani T. 2020. Factors influencing the presence of rodents in olive AeroSystems in southern Tunisia using occupancy models. J Anim Plant Sci. 44(3):7717–7726. https://doi.org/10.35759/JAnmPlSci.v44-3.4

Fares W et al. 2020. Co-circulation of toscana virus and *Leishmania infantum* in a focus of zoonotic visceral leishmaniasis from central Tunisia. Acta Trop. 204(2020):105342. https://doi.org/10.1016/j.actatropica.2020.105342

Ghatee MA, Sharifi I, Mohammadi N, Moghaddam BE, Kohansal MH. 2023. Geographical and climatic risk factors of cutaneous leishmaniasis in the hyper-endemic focus of Bam County in southeast Iran. Front Public Health. 11 (2023):1236552. https://doi.org/10.3389/fpubh.2023.1236552

Goodchild MF. 2007. Citizens as sensors: the world of volunteered geography. GeoJournal. 69(4):211–221. https://doi.org/10.1007/s10708-007-9111-y

Gorelick N. 2013. Google earth engine. EGU General Assembly Conference Abstracts, 2003; Vienna, Austria. Vol. 15. p 11997.

Haddad M, Nassar D, Shtaya M. 2023. Heavy metals accumulation in soil and uptake by barley (*hordeum vulgare*) irrigated with contaminated water. Sci Rep. 13(1):4121. https://doi.org/10.1038/s41598-022-18014-0

Jain S et al. 2023. Global leishmaniasis surveillance updates 2023. 3: years of the NTD road map. World Health Organ. URL: https://iris.who.int/bitstream/handle/10665/379491/WER9945-653-669.pdf?sequence=1

Jarallah HM, Aabadi HI, Shaalan NN. 2022. Environmental risk factors associated with distribution of visceral leishmaniasis in marshlands of Iraq. In: AIP conf Proc; 2022; [location]. Vol 2386(1), AIP Publishing LLC; p 020031. https://doi.org/10.1063/5.0067057

Kalitsilo L, Oronje R, Mbeye NM. 2025. Vector-borne disease control and management in irrigation areas: a neglected critical phenomenon in Malawi. Trop Med Infect Dis. 10(9):251. https://doi.org/10.3390/tropicalmed10090251

Karmaoui A et al. 2023. Thirty years of change in the land use and land cover of the ziz oases (pre-sahara of Morocco) combining remote sensing, GIS, and field observations. Land. 12(12):2127. https://doi.org/10.3390/land12122127

Karmaoui A, Sereno D, El Jaafari S, Hajji L. 2022. Seasonal patterns of zoonotic cutaneous leishmaniasis caused by *L. major* and transmitted by *Phlebotomus papatasi* in the North Africa region: a systematic review and meta-analysis. Microorganisms. 10(12):2391. https://doi.org/10.3390/microorganisms10122391

Kmoch L, Bou-Lahriss A, Plieninger T. 2024. Drought threatens agroforestry landscapes and dryland livelihoods in a North African hotspot of environmental change. Landsc Urban Plann. 245(2024):105022. https://doi.org/10.1016/j.landurbplan.2024.105022

Mili AF et al. 2012. Retrospective analysis of leishmaniasis in central Tunisia: an update on emerging epidemiological trends. Curr Trop Med Rep Chapter. 15:227–251. https://doi.org/10.5772/27250

Olmeda P et al. 2024. Twenty-year evolution of *Leishmania infantum* infection in dogs in Valdeorras (Galicia, Northwestern Spain): implication of climatic factors and preventive measures. Parasit Vectors. 17(1):281. https://doi.org/10.1186/s13071-024-06357-8

Orshan L et al. 2016. Distribution and dispersal of *Phlebotomus papatasi* (Diptera: psychodidae) in a zoonotic cutaneous leishmaniasis focus, the northern Negev, Israel (Diptera: Psychodidae) in a zoonotic cutaneous

leishmaniasis focus, the Northern Negev, Israel. PLoS Neglect. Trop. Dis. PLOS Neglected Trop Dis. 10(7). https://doi.org/10.1371/journal.pntd.0004819
Potere D. 2008. Horizontal positional accuracy of Google Earth's high-resolution imagery archive. Sensors. 8 (12):7973–7981. https://doi.org/10.3390/s8127973
Quan C, Han S, Utescher T, Zhang C, Liu YSC. 2013. Validation of temperature–precipitation based aridity index: paleoclimatic implications. Palaeogeogr Palaeoclimatol, Palaeoecol. 386(2013):86–95. https://doi.org/10.1016/j.palaeo.2013.05.008
Quan C, Liu YS, Tang H, Utescher T. 2014. Miocene shift of European atmospheric circulation from trade wind to westerlies. Sci Rep. 4(1):5660. https://doi.org/10.1038/srep05660
Ready PD. 2013. Biology of phlebotomine sand flies as vectors of disease agents. Annu Rev Entomol. 58(1):227–250. https://doi.org/10.1146/annurev-ento-120811-153557
Salah AB, Kamarianakis Y, Chlif S, Alaya NB, Prastacos P. 2007. Zoonotic cutaneous leishmaniasis in central Tunisia: spatio–temporal dynamics. Int J Epidemiol. 36(5):991–1000. https://doi.org/10.1093/ije/dym125
Shadomy SV et al. 2025. Emerging and re-emerging disease threats in the middle East and North Africa region—One Health approaches and potential strategies. Eur J Public Health. 35(Supplement_1):i3–i5. https://doi.org/10.1093/eurpub/ckae122
Shirzadi MR et al. 2020. Impact of environmental and climate factors on spatial distribution of cutaneous leishmaniasis in northeastern Iran: utilizing remote sensing. J Arthropod Borne Dis. 14(1):56–67. https://doi.org/10.18502/jad.v14i1.2704
Slimane TB et al. 2014. An investigation on vertical transmission of *Leishmania infantum* in experimentally infected dogs and assessment of offspring's infectiousness potential by xenodiagnosis. Vet Parasitol. 206(3–4):282–286. https://doi.org/10.1016/j.vetpar.2014.10.020
Tabbabi A. 2019. Review of leishmaniasis in the middle East and North Africa. Afr Health Sci. 19(1):1329–1337. https://doi.org/10.4314/ahs.v19i1.4
Tabbabi A, Ghrab J, Aoun K, Ready PD, Bouratbine A. 2011. Habitats of the sandfly vectors of *Leishmania tropica* and *L. major* in a mixed focus of cutaneous leishmaniasis in southeast Tunisia. Acta Trop. 119(2–3):131–137. https://doi.org/10.1016/j.actatropica.2011.05.002
Waitz Y, Paz S, Meir D, Malkinson D. 2019. Effects of land use type, spatial patterns and host presence on *Leishmania tropica* vectors activity. Parasit Vectors. 12(1):320. https://doi.org/10.1186/s13071-019-3562-0
World Health Organization. 2023. Global vector control response 2017–2030: progress report 2017–2022. World Health Organization. Available from: [accessed 2026 Jan 5]. https://www.who.int/publications/i/item/9789240060628
World Health Organization, Regional Office for the Eastern Mediterranean. 2025. Cutaneous leishmaniasis in Tunisia. [accessed 2026 Jan 5]. https://www.emro.who.int/neglected-tropical-diseases/countries/cl-tunisia.html
World Health Organization, UNEP United Nations Environment Programme, & World Organisation for Animal Health. 2022. One health joint plan of action (2022–2026): working together for the health of humans, animals, plants and the environment. World Health Organization.
Yu L, Gong P. 2012. Google Earth as a virtual globe tool for Earth science applications at the global scale: progress and perspectives. Int J Remote Sens. 33(12):3966–3986. https://doi.org/10.1080/01431161.2011.636081